Intrinsic luminescence centers in γ- and θ-alumina nanoparticles

Abdolvahab Amirsalari[1], Saber Farjami Shayesteh[1,†], and Reza Taheri Ghahrizjani[2,‡]

[1] *Nanostructures Labratory, Department of Physics, University of Guilan, Rasht, Iran*
[2] *Department of Physics, Optics and Laser Group, Shahreza Branch, Islamic Azad University, Isfahan, Iran*

(Received 25 June 2016; revised manuscript received 15 November 2016; published online 13 February 2017)

In this study, we investigate the photoluminescence (PL) properties of γ and θ-alumina nanoparticles synthesized by the chemical wet method followed by annealing. The obtained experimental results indicate the presence of some favorable near ultraviolet (NUV)-orange luminescent centers for usage in various luminescence applications, such as oxygen vacancies (F, F_2^+, F_2^{2+}, and F_2 centers), OH related defects, cation interstitial centers, and some new luminescence bands attributed to trapped-hole centers or donor–acceptor centers. The energy states of each defect are discussed in detail. The defects mentioned could alter the electronic structure by producing some energy states in the band gap that result in the optical absorption in the middle ultraviolet (MUV) region. Spectra show that photoionazation of F and F_2 centers plays a crucial role in providing either free electrons for the conduction band, or the photoconversions of aggregated oxygen vacancies into each other, or mobile electrons for electrons-holes recombination process by the Shockley–Read–Hall (SRH) mechanism.

Keywords: photoluminescence center, defect, oxygen vacancy, emission

PACS: 61.46.Hk, 78.55.Hx, 78.67.Bf, 81.07.Bc **DOI:** 10.1088/1674-1056/26/3/036101

1. Introduction

Alumina nanostructures have been the subject of many investigations due to their applications in many areas of modern industry such as electronics, metallurgy, optoelectronics, catalysts, and fine ceramic composites.[1] Alumina is an insulator material in the bulk state and has a band width of about 8.7–9.5 eV, whereas alumina nanostructures have shown different properties in comparison with their bulk state.[2–7] Some studies on alumina nanostructures and thin films have reported a decrease in the band gap width up to the semiconductor region due to the unsaturated and dangling bonds on the surface which can produce surface state energy levels and intrinsic energy levels in the band gap.[3,8–12] Sometimes, the density of defect energy levels (DELs) located in the band gap turns out to be so high that it supports the view of a split band gap.[3,12] For this reason some authors have inset alumina as an absorbance material[13] while some others as a transparent material in the wavelength range of 200–400 nm (MUV–NUV regions). There are more atoms on the surface of nanoparticles, and it is thus supposed that there exist more unsaturated and dangling bonds to produce different kinds of defects, which may increase the luminescence efficiency or appearance of new luminescence bands.[14,15] It is necessary to recognize different physical characteristics of each defect type, such as energy diagram, radiative and non-radiative decay mechanisms and their interactions with other defects for modification photonics and optoelectronics uses. Early observations of lattice damage, related optical coloration, and defect centers created by electron,[16,17] neutron,[18,19] and gamma[20] irradiation on alumina nanoparticles were carried out, and the characteristic of some defects such as F and F^+ centers was disclosed. However, these aspects including the nature of oxygen di-vacancies, cation interstitial, Frenkel cation and anion defects, excitons bound to defects, hole centers, and their interactions with the other traps have not been well studied. Thus, further theoretical and experimental investigations are needed.[20] Moreover, using a high dose of electron, neutron, or gamma irradiation to produce defects is not a safe method and will not be desirable for practical applications. Recently, we have used a simple but effective method to introduce a number of defects in alumina nanoparticles. In this study, anionic and cationic defective γ- and θ-alumina nanoparticles were synthesized using the precipitation method to investigate the structure of some electron centers such as F^+-, F-, F_2^{2+}-, F_2^+-, F_2-centers, cation interstitial centers, trapped-hole centers, and donor-acceptor centers. The positions of energy levels of the observed defects with respect to the bottom of the alumina conduction band have been investigated by considering photoluminescence (PL) and photoluminescence excitation (PLE) spectroscopies. The possible interaction of defects that can cause energy or charge transfer processes between the defects is also discussed.

2. Experimental section

2.1. Materials

Aluminum nitrate nonahydrate ($Al(NO_3)_3{\cdot}9H_2O$, 98.99 purity) was used as a precursor. 25% ammonia solution (99.00% purity) is obtained from Merck Inc, as a precipitant.

†Corresponding author. E-mail: saber@guilan.ac.ir
‡Corresponding author. E-mail: Taheri.reza@iaush.ac.ir

© 2017 Chinese Physical Society and IOP Publishing Ltd

2.2. Synthesis method

Alumina nanoparticles were prepared by the chemical wet method. Accordingly, aluminum nitrate was used as a precursor. The desired amount of aluminum nitrate was dissolved in deionized water, until 0.1 M $Al(NO_3)_3{\cdot}9H_2O$ solution is obtained. Then, the ammonia hydroxide solution (2 Mol/L) was added dropwise at a speed of 2 ml/min until a pH of 9.0 was achieved. The reaction was carried out at 60 °C for 60 min under constant mechanical stirring. As a result, the gel of aluminum hydroxide was obtained. The prepared gel was allowed to cool at room temperature for 1 h and then centrifuged and washed several times with deionized water to remove unreacted ammonia and nitrate. The samples were dried for 10 h at 110 °C with a temperature step of 5°/min in an oven and then grinding them. The prepared particles were calcined at varying temperatures of 550, 750, and 950 °C for 4 h with a temperature step of 10°/min.

2.3. Sample characterization methods

2.3.1. XRD

The XRD was performed on a PW 1840 diffractometer Philips (using Cu $K_\alpha = 1.5418$ Å radiation), and a step size of 0.04 at a scan rate of 0.5°/min. A high efficiency one-dimensional detector (Lynx Eye type) operated in integration mode. The diffraction patterns were collected in the 2θ range of 4°–75°.

2.3.2. Scanning electron microscopy

The morphology of the samples was studied using a TESCAN VEGA SEM, operating at 30 kV in a vacuum. The SEM study was performed on powder samples.

2.3.3. PL and PLE spectroscopies

PL and PLE spectra were measured with a Perkin-Elmer LS-55 luminescence spectrometer, equipped with a xenon discharge lamp (9.9 W) pulsed at the line frequency; monochromators F/3 Monk-Gillieson type, and 1 cm×1 cm pellet samples. In all experiments, excitation and emission slits were kept at 15 nm and 5 nm, respectively. PL and PLE spectra dissolved into bands by Gaussian fitting using OriginPro 8.1 software.

3. Results and discussion

3.1. Structural analysis

To study the effect of calcination temperature on the structural properties of alumina nanoparticles, a sample of $Al(OH)_3$ was divided in three parts and then calcined at various temperatures (550, 750, and 950 °C) for 4 h in air. The structural characteristics of samples with calcining treatment are shown in Fig. 1. The diffraction lines of samples calcined at 550 °C and 750 °C were strictly matched to the standard diffraction lines of γ-Al_2O_3 phase (JCPDS NO. 048-0367) with unknown structure. Treatment at 950 °C showed a polymorph structure of alumina consisting of θ-Al_2O_3 (JCPDS No. 047-1771), γ-Al_2O_3 and α-Al_2O_3 with very broad diffraction peaks, indicating a small crystallite size. θ-alumina was the dominant phase at this temperature. Some diffraction lines corresponding to γ-Al_2O_3 and α-Al_2O_3 were observed in the nanoparticles calcined at 950 °C as a fingerprint of these phases. The crystallite sizes of the synthesized nanopowders with annealing treatment and the phase evolution of the nanoparticles were estimated and listed in Table 1.

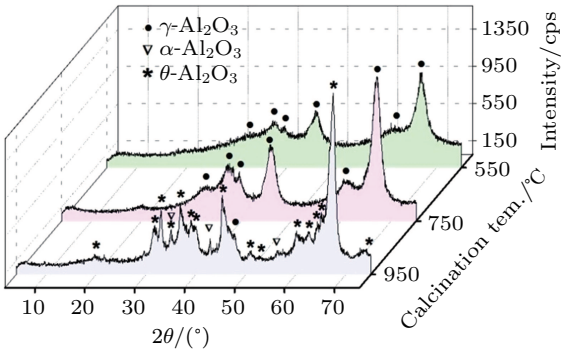


Fig. 1. (color online) XRD patterns of Al_2O_3 nanoparticles of various phases obtained by calcinations.

Table 1. Characteristic properties of alumina nanoparticles calcined at different temperatures (the crystallite size was determined from the first highest intensity diffraction peak located at $2\theta \approx 67°$).

Calcinations temperature/°C	Phase composition	Crystallite size/nm
550	$\gamma-Al_2O_3$	3.2
750	$\gamma-Al_2O_3$	4.2
950	A polymorph structure containing α, γ and $\theta-Al_2O_3$. θ-alumina is the dominant phase	5.6

3.2. Morphology study

The morphology of the samples was investigated by scanning electron microscope (SEM) as shown in Fig. 2. All three samples showed nanoparticles in the range of 22–46 nm, which were not distributed uniformly. However, a number of larger particles with a diameter beyond 50 nm can be clearly seen in all images (regions surrounded by purple lines). The presence of the agglomerated particles may be due to the large specific surface area of nanoparticles, which makes them thermodynamically unstable and tend to agglomerate.

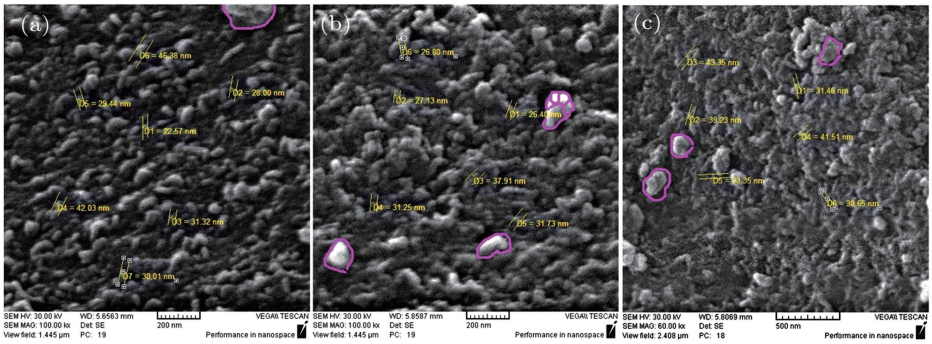


Fig. 2. (color online) SEM images of alumina nanoparticles calcined at (a) 550 °C, (b) 750 °C, and (c) 950 °C.

3.3. Optical studies

3.3.1. Photoluminescence spectra of Al_2O_3 nanoparticles with change in excitation wavelength

Figure 3 shows the PL spectra of alumina nanoparticles with changes in excitation wavelength. The PL spectra were strongly dependent on excitation wavelength. There were 14 luminescence bands in the PL spectra of samples in the wavelength range of 1.9–3.54 eV with an excitation of $\lambda_{ex} = 200$ nm (6.2 eV). The intensity of some emission bands were decreased and some others are quenched with increasing excitation wavelength from 200 nm (6.2 eV) to 350 nm (3.54 eV). For excitation wavelength higher than 240 nm (5.17 eV), the intensity of the emission bands at 3.05, 2.47, 2.42, and 2.33 eV were negligible and also the emission bands centered at 2.83 and 2.10 eV were completely quenched. The excitation bands of aforementioned emissions were located at excitation wavelengths less than 240 nm (5.17 eV). For detecting more defect centers, the excitation wavelength was selected at $\lambda_{ex} = 200$ nm.

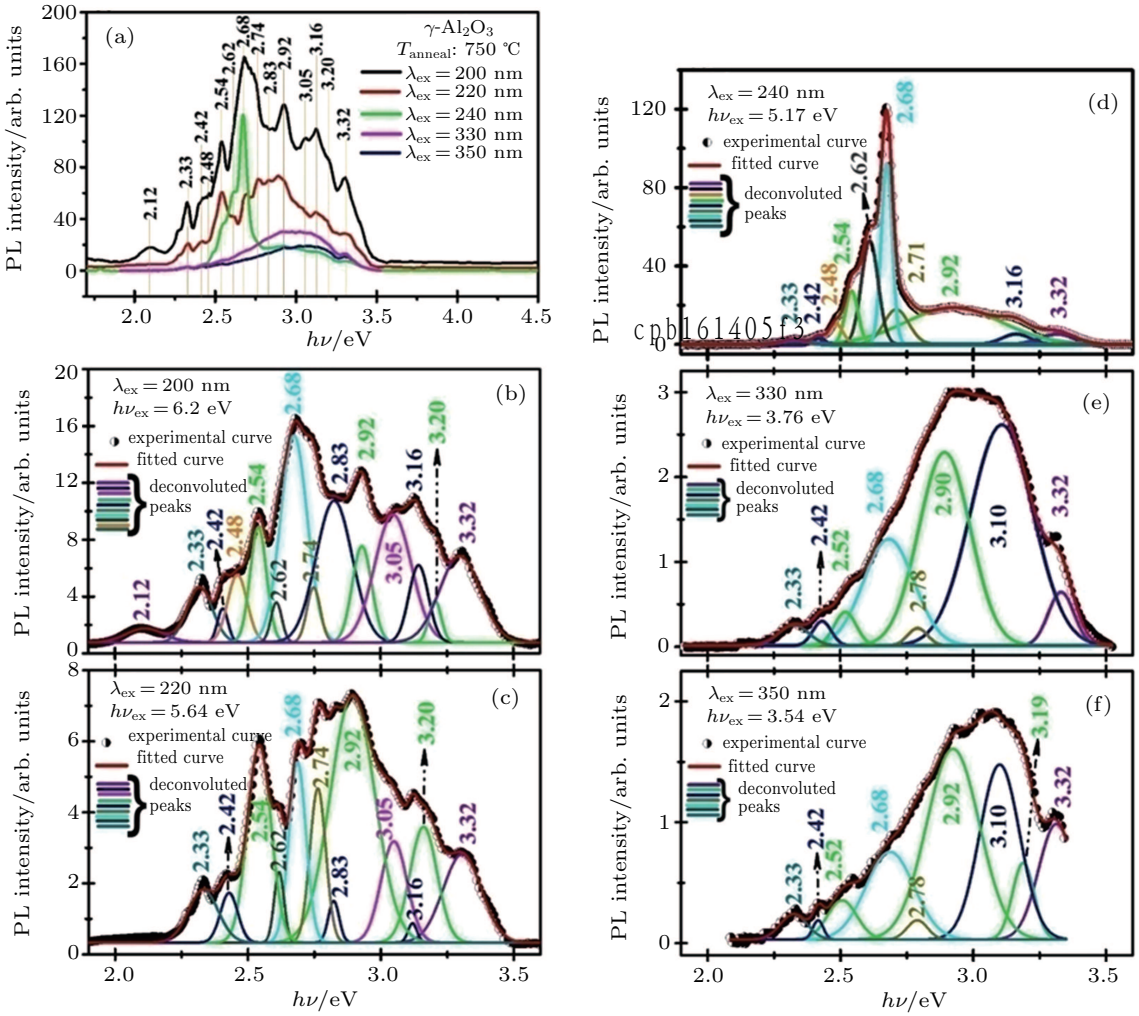


Fig. 3. (color online) PL spectra of Al_2O_3 nanoparticles calcined at 750 °C in air with different excitation wavelengths.

3.3.2. Calcination temperature on photoluminescence properties of Al_2O_3 nanoparticles

The PL emission spectra and deconvoluted luminescence bands of Al_2O_3 nanoparticles prepared at different calcination temperatures with an excitation wavelength of 200 nm (6.2 eV) at room temperature are shown in Fig. 4. All the samples showed emissions at 3.32, 3.19–3.20, 3.10–3.16, 3.02–3.09, 2.92, 2.83, 2.74, 2.68, 2.63, 2.54, 2.47, 2.42, 2.33, and 2.10–2.13 eV. The excitation bands of these emissions are presented in Fig. 5(b)–5(n) for the γ-Al_2O_3 sample annealed at 750 °C (other samples have similar PLE spectra). In the description given below, the origin of various observed luminescence bands is discussed.

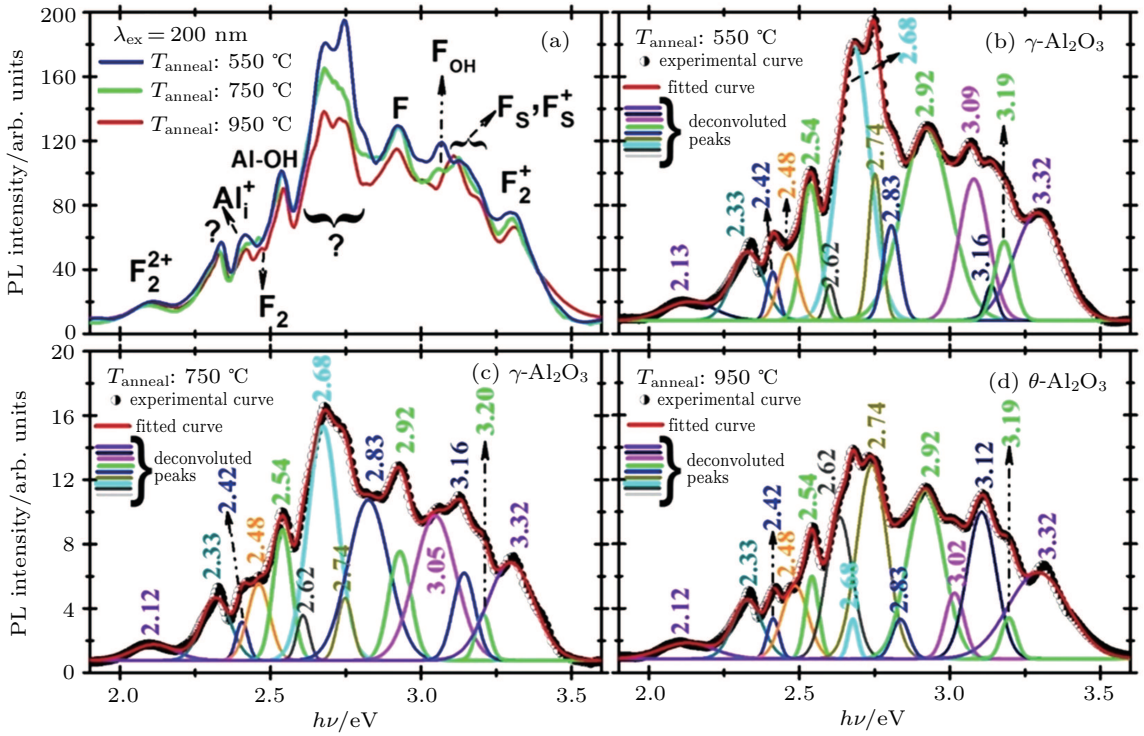


Fig. 4. (color online) (a) Photoluminescence spectra of different calcinated alumina nanopowders measured under excitation wavelength of 200 nm (6.2 eV) at room temperature. (b)–(d) Deconvoluted luminescence bands of nanopowders calcinated at different temperatures.

i) Emission bands related to F centers It was reported that F centers have emission and absorption bands at about 2.91–3.02 eV and 6.05 eV, respectively.[11,19,21]

From theoretical calculations, the excited states of the F center corresponding to 1B, 2A, and 2B states are located approximately at the same position (three low lying excitations always appear in a narrow range of energy) near or into the conduction band edge.[11,20,22] The F center is analogous to the helium atom. The ground state is therefore $(1s)^2{}^1S$, and possible excited states are (1S)(2S) ^1S, ^3S and (1S)(2P) ^1P, ^3P. The only allowed transition is $^1S \rightarrow {}^1P(^1A_{1g} \rightarrow {}^1T_{1u})$. The $^1S \rightarrow {}^1P$ transitions in alumina give rise to the 6.05 eV absorption band.[23] As far as the emission transitions are concerned, the $^1P \rightarrow {}^1S$ (fast component, singlet-singlet) transition is allowed, and the $^3P \rightarrow {}^1S$ transition (slow component, triplet–singlet), although spin-forbidden, may also be allowed due to spin–orbit admixture of ^3P and ^1P.[23] Although triplet–singlet transition is a spin-forbidden transition, it has commonly been observed in alumina materials due to the strong spin–orbit admixture of ^3P and ^1P. This predicted a negligibly small Stokes shift for the $^1P \leftrightarrow {}^1S$ transition, which is in sharp disagreement with the experiment.[23] In addition, from the experimentally determined Huang–Rhys factor,[24] $S = 14.7$, the Stokes shift of the emission band from the 6 eV absorption band was expected to be 1.23 eV instead of the observed ~ 3.1 eV, showing a large disagreement.[11] These results were interpreted by assuming that the slow luminescence originated from a triplet state following ~ 1.8 eV non-radiative relaxation from the relaxed singlet excited state.[25]

The absorption and emission diagrams of these centers are illustrated in Fig. 8. As shown in Fig. 5(e), the PL component at 2.92 eV which has a side excitation band ended to 6.2 eV was related to F centers.[11,26]

Moreover, the emission band at 3.09 eV for the sample calcined at 550 °C having only a side excitation band centered at 5.99 eV (Fig. 5(d)) was believed to be ascribed to the F centers, but another kind of F centers was probably perturbed by OH ions or other phenomena. The behavior of this emission band was also similar to the 2.92 eV luminescence band because of excitation and emission bands at 5.99 eV and 3.02–

3.09 eV respectively. In addition, the presence of different kinds of F centers in transition-alumina has been established previously.[27] The reason is that in crystalline nanoparticles, most defect states are sensitive to the positions of nearby atoms or ions, so that the formation of the absorption and the energy position of the emission depend on the vibrations of the surrounding ions.

ii) Emission band related to F_2^+ centers As can be seen from Fig. 5(b), the emission band at ~ 3.32 eV has three excitation bands centered at 6.13 eV, 5.28 eV, and 3.56 eV.

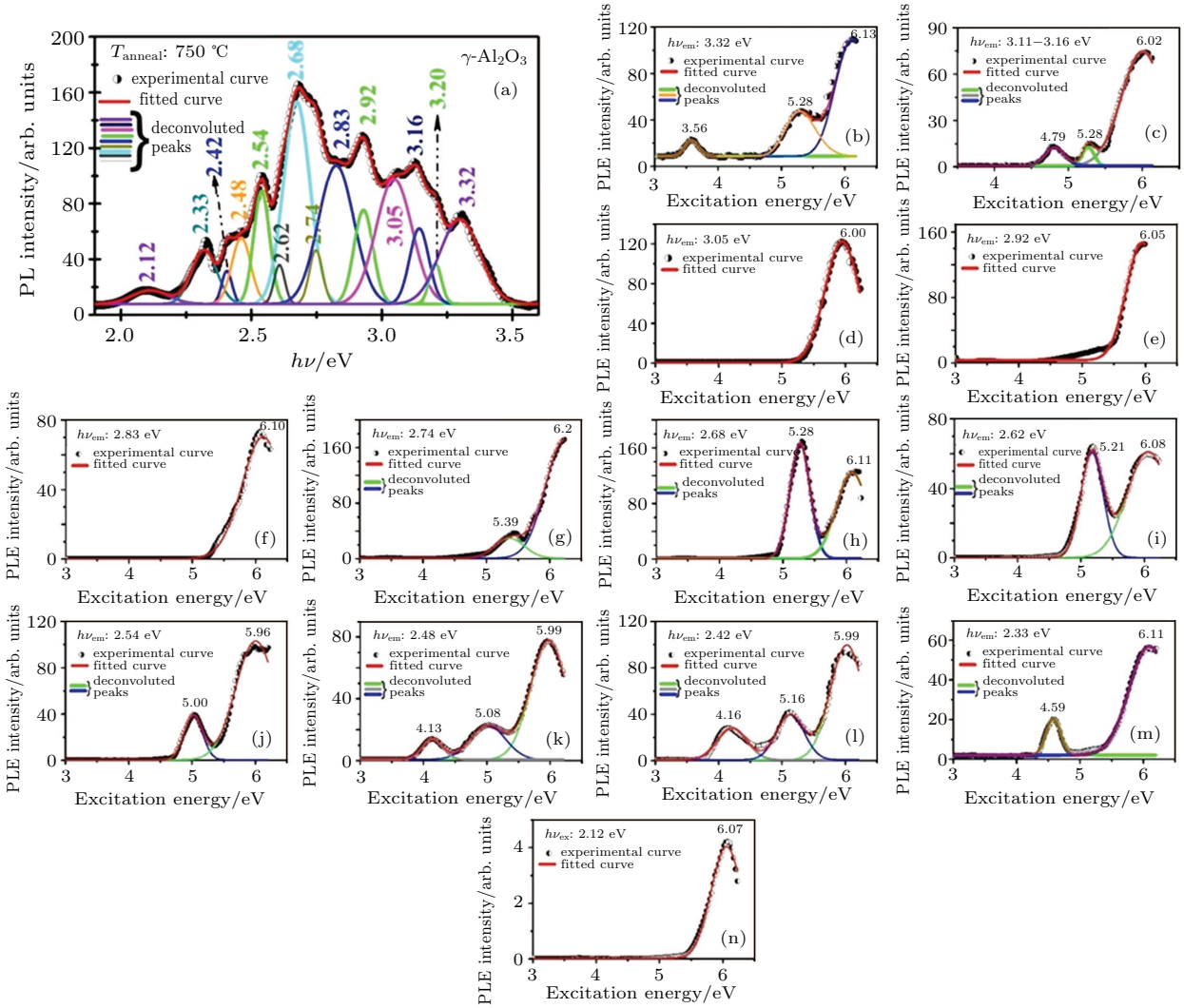


Fig. 5. (color online) (a) PL emission spectrum with deconvoluted luminescence bands of alumina nanoparticles calcined at 750 °C. Panels (b)–(n) correspond to PLE spectra of alumina nanoparticles detected at $h\nu_{em} = 3.32$, 3.16, 3.05, 2.92, 2.83, 2.74,2.68, 2.62, 2.54, 2.48, 2.42, 2.33, and 2.12 eV, respectively.

As illustrated in Fig. 8, singlet-singlet transitions in the F centers and ICTs in F_2^+ centers (F_2^+ center: two anion vacancies with three trapped electrons) give rise to an emission band in this region[11,28] (ICTs: intra-center electronic transitions, electronic transition between the ground and excited states of the defect, GCTs: electronic transition from the ground state of the defect center to conduction band). It is supposed that this band was not related to singlet-singlet transitions in the F centers because these centers could not be excited at excitation wavelengths higher than 260 nm (4.77 eV), while this emission band was detected in the Pl spectrum excited at $\lambda_{ex} = 350$ nm. This emission band was supposed to be caused by ICTs in the F_2^+ centers.[28,29] 3.56 eV and 5.28 eV excitation bands were caused by ICTs in the F_2^+ centers and photo-conversions of F_2^{2+} to F_2^+ centers, respectively.[11,30–34] It has been demonstrated that a quantum photo excitation energy higher than 5 eV ($\sim h\nu \geq 5$ eV) can dissociate an electron from an F_2 center to release into the conduction band.[11,30] 5.28 eV excitation energy was supposed to release an electron of F_2 center to the conduction band and then this electron would be trapped by an F_2^{2+} center and a photon at 3.32 eV would be emitted in the following reactions:[20,29]

$$F_2 + (4.96\ \text{eV}) \rightarrow F_2^+ + e_{CB}^-, \quad (1)$$

$$e_{CB}^- + F_2^{2+} \rightarrow (F_2^+)^* \rightarrow F_2^+ + h\nu(3.32\ \text{eV}), \quad (2)$$

where e_{CB}^- is denoted as an electron in the conduction band and $(F_2^+)^*$ stands for F_2^+ in an excited state. Because of the aforesaid reason, an excitation band was observed at 5.28 eV in

the PLE spectrum of Al_2O_3 nanoparticles detected at $h\nu_{em} = 3.32$ eV. A similar scenario was done for the side excitation band centered at 6.13 eV. It has been established that the excited levels of the F center lie at the conduction band edge. Therefore, F centers can act as a source of free electrons for the conduction band at excitation of 6.1 eV, i.e.,[20,33,35]

$$F + h\nu(6.1\ \text{eV}) \rightarrow F^+ + e^-_{CB}. \quad (3)$$

Then, e^-_{CB} can be trapped by an F_2^{2+} center and scenario (2) is repeated. Because of the aforementioned reason, a side excitation band centered at 6.13 eV was also observed in the PLE spectrum detected at 3.32 eV.[29,30]

iii) Emission band related to Al–OH The emission band at 2.54 eV that had two excitation bands centered at 5.96 eV and 5 eV was attributed to the hydroxyl group bound to a surface aluminum ion. The samples with a large specific surface may have surface defects, such as hydroxyl group bound to surface aluminum ions (Al–OH), which also contribute to the luminescence process, providing an emission band at about 2.54 eV.[36]

iv) Emission bands related to F_S^+ and F_S centers As illustrated in Fig. 5(c), the emission bands at 3.20 and 3.16 eV had three excitation bands at 6.02, 5.28, and 4.79 eV. The emission bands at 3.11–3.20 eV, which changed their positions with increasing calcination temperature and had a higher sensitivity to annealing temperature than the other ones, were attributed to F_S^+ or F_S centers (F or F^+ centers on nanostructure surface denoted as F_S or F_S^+, correspondingly[37,38]). Three excitation bands were matched to either of the three absorption bands of F^+ centers with a small shift or the absorption bands of F and F_2 centers by the following consideration. A theoretical study was performed on the optical transitions of F centers in the bulk and on the (0001) surface of α-alumina by first-principles methods. The effects of oxygen vacancies on the crystalline structure were determined by the appropriate atomic structure optimization carried out using a periodic model and density functional theory (DFT) calculations.[22] As a result of the theoretical study, three excitation states of both F and F^+ centers located on the surface of the crystal appeared in a wider range of energy in comparison with F and F^+ centers located in the bulk of the material. The energy of the first excitation band (the band at 4.79 eV, in PLE spectra detected at $h\nu_{em} = 3.16$ eV) of 3.11–3.20 eV emission bands in the present work, was analogous to 1A→2A allowed transitions of the calculated surface F centers (4.62 eV).[22] The other two excitation bands (6.02 and 5.28 eV) might be caused by photo-conversion of F_S^+ to F_S centers. As mentioned previously, F and F_2 centers could release electrons into the conduction band when excited at 6.05 and 5.28 eV, respectively. Then the free electrons could migrate through the material and eventually would be captured by F_S^+ centers and produce $(F_S)^*$ centers, providing an emission band at 3.1–3.20 eV. However, in the case of F centers located on the surface, the situation is more complex since the absorption and emission bands are strongly affected by the sample history and the environment.

v) Emission bands related to F_2 centers As illustrated in Fig. 8, F_2 center (i.e., two oxygen vacancies with four trapped electrons) has an absorption and two emission bands centered at 4.09 eV, 3.85 eV, and 2.4 eV, respectively. Moreover, a quantum photoexcitation energy higher than 4.8 eV could completely dissociate an electron of this center corresponding to GCT.[11,19,28,39] 2.42 eV emission that has three excitation bands centered at 4.16 eV, 5.16 eV, and 6.05 eV was supposed to attribute to F_2 centers. The first excitation band corresponds to ICTs in F_2 centers and the two others were caused by photoionization of F (and/or F_2^+) and F_2 centers and finally conversions of $F_2^+ \rightarrow F_2$ centers. The excitation energy higher than 6.05 eV and 5 eV has the capability to dissociate electrons from the F and F_2 centers, respectively, and ionize them. Finally, the free electrons would migrate through the material and would eventually be captured by F_2^+ centers, corresponding to the following reactions:[11,20]

$$F_2 + h\nu(4.96\ eV) \rightarrow F_2^+ + e^-_{CB}. \quad (4)$$

e^-_{CB} could go back and be trapped by its ionized center or migrate and finally was captured by an F_2^+ center that would trigger a recombination mechanism to yield an emission of 2.42 eV by following the scheme[20]

$$F_2^+ + e^-_{CB} \rightarrow (F_2)^* \rightarrow F_2 + h\nu(2.42\ \text{eV}). \quad (5)$$

From this point of view, 5.16 eV excitation energy gave rise to an emission band at 2.42 eV. The 6.05 eV excitation band was caused by the following reactions:[20,33]

$$F + h\nu(6.05\ \text{eV}) \rightarrow F^+ + e^-_{CB}, \quad (6)$$

$$F_2^+ + e^-_{CB} \rightarrow (F_2)^* \rightarrow F_2 + h\nu(2.42\ \text{eV}). \quad (7)$$

vi) Emission bands related to interstitial aluminum ions The emission band at 2.48 eV could be related to interstitial aluminum ions or perturbed aggregate F_2 centers. The optical transitions of free Al^o, Al^+, and Al^{2+} in the energy range from 3 to 7.5 eV can shift to lower energies when these ions are incorporated into the interstitial sites of Al_2O_3. Interstitial aluminum ions can act as simple donor centers.[18,40] Interstitial Al_i^+ center has three absorption bands at 3.8 eV, 2.95 eV, and 4.1 eV and an emission band centered at 2.45 eV.[18] It seems reasonable to propose a hypothesis that 2.48 eV emission having three excitation bands centered at 4.13 eV, 5.99 eV, and 5.08 eV was due to interstitial Al_i^+ ions. The first excitation band (4.13 eV) was due to electronic transition from the ground state to excited states of these centers. There are two possible scenarios to explain the observed excitation band of 5.99 eV. In the first scenario, this exciting band was caused

by near simultaneous excitations of F and interstitial Al_i^+ centers. Since the emission band of the F centers was located at 2.92 eV it was near the excitation band of the Al_i^+ centers. At a quantum excitation energy of ≈ 5.99 eV, the F center was excited and a photon of 2.92 eV would emit (the time interval between excitation and emission is of the order of milliseconds). Then an electron of the Al_i^+ center would absorb this emitted photon and use the energy to jump to an excited energy level, returning the Al_i^+ center to the ground state. This was accompanied by the emission of a photon at ~2.48 eV, as illustrated in Fig. 6. For this reason, an exciting band centered at 5.99 eV was observed in PLE spectrum detected at 2.48 eV.

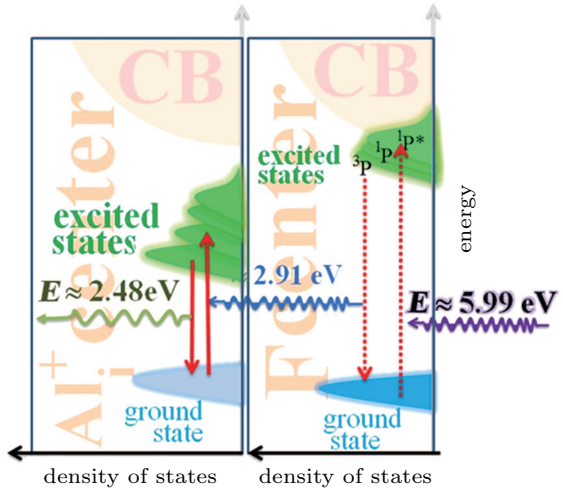


Fig. 6. (color online) The schematic energy diagram for the ~ 5.99 eV absorption band of emission at 2.48 eV. The F center absorbed a photon ($h\nu \approx 5.99$ eV) and would emit at 2.91 eV. Then Al_i^+ center would absorb emitted photon (2.91 eV) to emit at 2.48 eV (since the energy of the emitted photon from the F center and the absorption energy of Al_i^+ center were very close together).

In the second scenario, the free electron produced by photo-ionization of the F center was trapped in the Al_i^{2+} center. This process would produce an excited state of the Al_i^+ center by conversion of $Al_i^{2+} \rightarrow Al_i^+$ to yield a photoemission of 2.48 eV by returning the Al_i^+ center from the excited state to the ground state.[41] The third excitation band may have been caused by photoionization of F_2 centers, where the free electron was created as the photoexcited electron left the F_2 center. The free electron would eventually be captured by the Al_i^{2+} center, corresponding to the following reactions:[20]

$$F_2 + (5.08\ \text{eV}) \rightarrow F_2^+ + e_{CB}^-, \quad (8)$$

$$e_{CB}^- + Al_i^{2+} \rightarrow (Al_i^+)^* \rightarrow Al_i^+ + h\nu(2.48\ \text{eV}). \quad (9)$$

It is likely that a quantum photoexcitation energy of $\sim h\nu \geq 5$ eV could dissociate an electron from the Al_i^+ center to release into the conduction band, and then the free electron would be trapped by other isolated Al_i^+ center (Al_i^{2+} center), providing an excited state of the Al_i^+ center. Taking into account the experimental data of this work and also the results of previous research propose an energy level diagram for the Al_i^+ center.[18,20]

vii) Emission bands related to F_2^{2+} centers It has been reported that F_2^{2+} centers (two oxygen vacancies with two trapped electrons) have absorption and emission bands centered at 2.75 eV and 2.13–2.2 eV, respectively.[11,19,39] Hence, it is believed that the emission centered at 2.12 eV having a side excitation band centered at 6.07 eV may be due to F_2^{2+} centers perturbed by neighboring ions for the following considerations.

This luminescence band was only observed in the PL spectrum excited at $\lambda_{ex} = 200$ nm (6.2 eV). This center was approximately quenched at an excitation wavelength higher than 200 nm (see Fig. 5, there is no luminescence line at 2.12 eV for the samples excited at $\lambda_{ex} = 220$–370 nm). It was illustrated by Ikeda *et al.*[20] that excitation energy lower than 5.2 eV could not ionize F_2^+ centers due to the nature of the deep trap. On the other hand, it was almost the most important source for producing the F_2^{2+} center in high energy irradiations. If the excitation energy was not large enough to ionize F_2^+ centers, but was large enough to ionize F_2 centers (5 eV$\leq h\nu <$ 6.2 eV), then the following phenomenon could occur.

The dissociated electrons from F_2 centers would be trapped by F_2^{2+} centers, which could lead to conversion of F_2^{2+} centers to F_2^+ centers with emission of photons at 3.32 eV. The luminescence band at 2.13–2.1 eV would be vanished by this phenomenon due to the conversion of the entire F_2^{2+} centers to F_2^+ centers. This condition is called complete photoconversion and expressed as follows:

$$\text{at} \quad 5\ \text{eV} \leq h\nu < 6.2\ \text{eV} \Rightarrow F_2 + h\nu \rightarrow F_2^+ + e_{CB}^-, \quad (10)$$

and then

$$e_{CB}^- + F_2^{2+} \rightarrow (F_2^+)^* \rightarrow F_2^+ + h\nu(3.32\ \text{eV}). \quad (11)$$

At excitation energy $(h\nu) \geq 6.2$ eV, although a fraction of the F_2^{2+} centers was virtually wiped out by the electron–F_2^{2+} center capturing processes, the optical ionization of F_2^+ centers would reproduce it. Hence, a balance was created between conversions of $F_2^+ \leftrightarrow F_2^{2+}$ centers. In this process, the luminescence bands of both defects would be observed. This process can be described using the following formula:[20]

$$\text{at} \quad 6.2\ \text{eV} \leq h\nu \Rightarrow F_2^+ + h\nu \rightarrow F_2^{2+} + e_{CB}^-. \quad (12)$$

Here, e_{CB}^- may be trapped by other defects. The important phenomenon that most probably occurred was that the produced F_2^{2+} centers may absorb 2.92 eV emitted photons from F centers and would re-emit them at 2.12 eV, as illustrated in Fig. 7. These explanations interpret the silence of 2.12 eV emission at excitation wavelengths longer than 6.07 eV (F_2^{2+} centers could capture electrons and virtually wiped out at exciting energy

lower than 6.07 eV, while reproduction would be possible at exciting energy higher than 6.07 eV due to ionization of F_2^+ centers).

viii) The well localized F^+ center emission band According to theoretical and experimental measurements, the well localized F^+ centers have three absorption bands attributed to 1A→1B (4.8 eV), 1A→2A (5.2–5.4 eV), and 1A→2B (5.9–6.3 eV) transitions.[11,21,28] Indeed, in the F^+ centers, excitations are sensitive to the light polarization where 1A → 2A corresponds to an excitation with light polarized in the direction perpendicular to the *c* axis, and the 1A → 1B and 1A → 2B appear when the exciting light is polarized in a direction parallel to *c*.[11,21,23] Also, F^+ center excitation states (1B, 2A, and 2B) are rather well separated.[22] The luminescence of this center stands for the transition from the relaxed, lowest excited state to the ground state, 1B→1A.

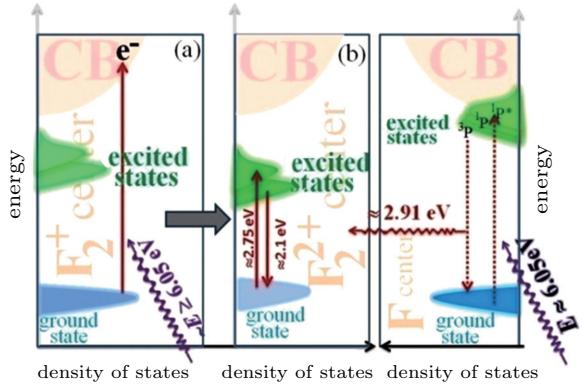


Fig. 7. (color online) The schematic energy diagram for the luminescence band at 2.12 eV in a two-photon absorption process. A photon was absorbed and took the F_2^+ system from state (a) to state (b). Another photon was absorbed by F center and a photon at 2.92 eV would be emitted. Then the new system of F_2^{2+} would absorb the 2.92 eV emitted photon to emit a photon at 2.1 eV, since the energy of the emitted photon from the F center and the absorption energy of the F_2^{2+} center were very close together.

Figure 8 shows the illustrated diagram of its transitions in alumina. It must be mentioned about alumina nanostructures that there are two different types of F^+ centers. F^+ centers located on the surface of the nanostructures are denoted as F_S^+ centers with an emission of 3.1–3.2 eV[37,38] (as previously discussed) and F^+ centers that are located in the bulk of nanostructures have a similar trend to F^+ centers in the bulk materials with an emission band of 3.8 eV.[11,21,28,42] Because in this situation the electron orbitals are well localized, the emission band of 3.16–3.20 eV having three excitation bands at 4.79, 5.28, and 6.02 eV attributed to F_S^+ centers was detected, but it was not observed in the emission band at 3.8 eV, which could be attributed to well localized F^+ centers due to the following considerations. It is possible that all F^+ centers were located on the surface of nanoparticles to give rise to an emission of 3.1 eV because these centers were more sensitive to annealing temperature. If there were well localized F^+ centers in the bulk of nanoparticles, then the relaxation process would be constituted by "non-radiative transitions", the mechanism of non-irradiation excitation transfer between closely located F^+ and F centers would be likely to take place or the mechanism of possible "electron tunneling from F^+ to F centers" was likely to occur due to the following reactions:[33,43]

$$(F^+)^* + F \rightarrow F^+ + F^* \tag{13}$$

$$(F^+)^* + F \rightarrow F^+ + F^* \rightarrow F^+ + F + h\nu\ (3\ \text{or}\ 3.23\ \text{eV}) \tag{14}$$

$$(F^+)^* + F \rightarrow F^+ + (F)^* \rightarrow F^+ + F^+ + e_{CB}^-. \tag{15}$$

In addition, in nanocrystals with a high concentration of F centers, the mechanism of electron transport by tunneling between F and F^+ centers may occur. Some of the single-vacancy centers are not completely isolated, but are closely located to each other, forming a weakly coupled F type center pair, e.g., F + F, F +F^+, and F^++F^+ pairs. Although the positively charged F type centers (like F^+, F_2^+ and F_2^{2+} centers) are likely to be the candidates for the trapping centers, weakly coupled pairs are responsible for the electron tunneling process.[44,45] The probability for electron tunneling appears to strongly depend on the spin state character of the initial state.[46] The direct electron tunneling between F and F^+ centers may occur in one of two ways: it involves electron tunneling between their ground states or their excited states with a difference that the tunneling between their ground states is more slower than tunneling between excited states.[46] It was believed that the electron in triplet excited state of the F^+ center in a weakly coupled F +F^+ pair had a potential to tunnel to the triplet excited state of the F center without escaping to the conduction band to produce unstable forms of F^{2+}[31,47,48] and F^- centers[33,48,49] (F^{2+} and F^- denote bare oxygen vacancy and an oxygen vacancy with three trapped electrons, respectively). For the F^- center, the third electron being added to the F center was not localized by an oxygen vacancy but was shared mainly by the nearest Al atoms.[49] Hence, the ground state of the F center did not shift considerably whereas the additional electron occupying the local state is close to but below the conduction band edge. This delocalized electron of the F^- center has the potential to be trapped by other defects. It could be emitted from the nanocrystal or could tunnel into the conduction band and may be trapped by other F^+ centers to form an excited F center, which were relaxed by emitting a photon energy of 2.92–3 eV or 3.23 eV.[33]

$$(F^+)^* + F \xrightarrow[\text{tunneling}]{e} F^{2+} + F^- \rightarrow F^{2+} + F + e_{CB}(e_{trap}), \tag{16}$$

$$\text{then}\ \ e_{CB}(e_{trap}) + F^+ \rightarrow (F)^* \rightarrow F + h\nu(\approx 3\ \text{eV}\ \ \text{or}\ \ 3.23\ \text{eV}). \tag{17}$$

For the produced unstable F^{2+} center in the weakly coupled F+F^{2+} pair in Eq. (17), it immediately combined with one or

two stray electrons to form excited states of $(F^+)^*$ or $(F)^{**}$

$$e_{CB} + F^{2+} + F \rightarrow (F^+)^* + F, \quad (18)$$

$$2e_{CB} + F^{2+} + F \rightarrow (F)^{**} + F \rightarrow F + F + h\nu_1 + h\nu_2. \quad (19)$$

In the case of electron–F^{2+} center combination, a weakly coupled F+$(F^+)^*$ pair would be produced again. The relaxation process and emission energies of $(F)^{**}$ (both electrons of F center were placed in excited states) were believed to have a difference with the relaxation process of $(F)^*$ (an electron was placed in an excited state and the other in the ground state).

Although the electron tunneling from F^+ to F centers might have occurred, the reverse phenomenon, i.e. the electron tunneling from F to F^+ centers in alumina[46] was more common,

$$F^+ + (F)^* \xrightarrow[\text{tunneling}]{e} (F)^* + F^+ \rightarrow F + F^+ + h\nu(\approx 3\ \text{eV or } 3.23\ \text{eV}). \quad (20)$$

The phenomena discussed above might occur together. Hence the presence of well localized F^+ centers on the structure of the nanoparticles remained on the vague side.

ix) New luminescence bands attributed to V-type centers and various kinds of OH groups There were some new luminescence bands in PL spectra centered at 2.83, 2.74, 2.68, 2.62, and 2.33 eV, and their excitation bands were listed in Table 2.

Table 2. Characteristic properties of luminescence bands centered at 2.83, 2.74, 2.68, 2.62, and 2.33 eV.

Emission band/nm	Excitation bands/nm
2.83	6.10
2.74	6.2, 5.39
2.68	6.11, 5.28
2.62	6.08, 5.21
2.33	6.11, 4.59

There were speculations on the origin of these emissions. While the excitation regions of these new luminescence bands strongly matched with native point defects (F and F^+ centers), there was no accordance between characteristics of their emissions and reported F_2 type centers (F_2, F_2^+, and F_2^{2+} centers). While some authors attributed them to OH groups, the V type centers and hole trapped by interstitial oxygen (O_o^x) ions (trapped-hole centers)[50,51] could absorb light in the UV region to give rise to various luminescence bands in the NUV to visible region. Therefore, there were two assumptions about the origination of these new luminescence bands.

(i) The first one was related to hole centers, which are related to V-type centers or hole trapped by interstitial oxygen (interstitial O^-, O^o, and O^+ ions).[50,51] It has been established that the aluminum vacancies related to hole traps, i.e., V centers (a hole trapped on an oxygen ion forming an O^-, and two O^- were adjacent to an aluminum vacancy forming a V^- center), V^{2-} centers (a center comprised of an O^- adjacent to an aluminum vacancy) and V_{OH}^- centers (an OH^- ion adjacent to a V^{2-} center) act as trapping centers and have an absorption band near 3 eV. Also, such centers can absorb light in the UV region[32,34,52–54] (i.e. 3.1–4.1 eV). Due to the existence of different kinds of OH ions, more than one kind of V_{OH}^- centers may exist in the structure of alumina nanoparticles. In addition, trapped-hole centers in alumina are formed by trapping two and three holes at an interstitial anion. These may be indicted as interstitial O^o and O^+ ions.[50,51,55,56] The coinciding of excitation bands of such new luminescence bands with absorption bands of F type centers indicated that the luminescence were done by Auger recombination or trap-assisted recombination (Shockley–Read–Hall model, SRH model)[55–57] of dissociated electrons from F type centers to be captured by said hole centers (V^-, V^{2-}, V_{OH}^- centers, interstitial O^-, O^o, and O^+ ions) or another delocalized holes in the place of said hole centers.[32,33,43,55,56] It was suggested that these delocalized holes might be located on the surface or at interfaces between nano-crystallites. From this point of view, some luminescence bands in the blue–green region might be observed when we tuned the excitation wavelength around 6.05 eV and 5.21 eV (corresponding to the dissociation energy of an electron from F and F_2 centers, respectively). Irradiation in the 6.1 eV band led to the ionization of F centers, providing a source of electrons for the repopulation of the traps. The integrated intensities of these emission bands decreased (emission bands at 438–472 nm) with increasing calcination temperature from 550 °C to 950 °C due to a reduction in the number of the V_{OH}^- centers.

(ii) The other was related to different kinds of OH groups incorporated on the surface of nanoparticles responsible for these emissions.

The reported luminescence bands of OH^- species were strongly matched with the observed luminescence bands, but experimental data about their excitations showed a high dispersion. The exact nature of the OH species responsible for the fluorescence is not completely clear yet. However, it seems reasonable to assume that the OH groups are localized on the surface of alumina nanoparticles, which can be understood to have different local environments.[58]

This was the reason leading to the observed different luminescence bands in the blue-green regions of the spectrum. The photogenerated electron–hole pair was trapped in sites with a binding energy, such as =Al–OH groups, where the photoluminescence emission occurred.[58,59] If OH groups loses electrons due to excitation, then the deformed hydroxyl-group type is supplied. But if the photogenerated electron–hole pairs are trapped in these sites then their stability is maintained. So, it seems reasonable to assume that the free carriers

produced by photoionization F type centers would be trapped by a different kind of –OH species to cause luminescence. For this reason, the excitation spectra of these luminescence bands consist of a number of absorption bands of the F type centers. Moreover, the probability of the existence of various kinds of OH groups in alumina have been proved, Shen *et al.*[60] reported six types of OH species on the surface of alumina to cause luminescence in the range of 2.25–3.65 eV. Moreover, there are more reports about luminescence bands at about 3.02, 2.83, 2.74, 2.68, and 2.25 eV attributed to donor-acceptor on surface alumina.[58–61]

Taking into account the experimental data of the present study and also the results of other studies, we propose their energy diagrams by considering Pl and PLE spectroscopies, as illustrated in Fig. 8.

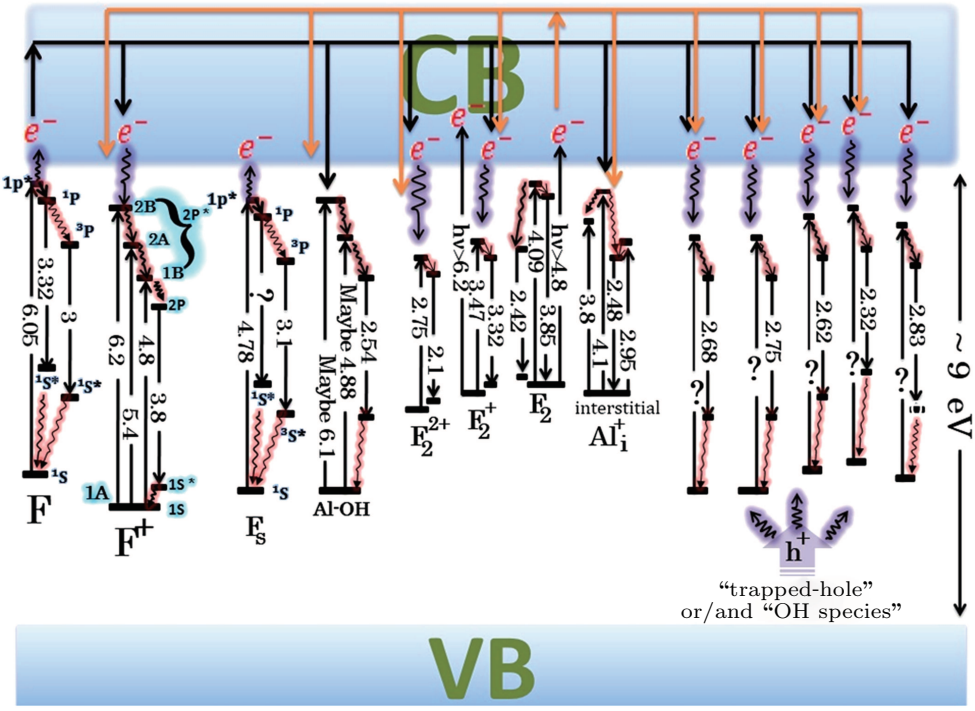


Fig. 8. (color online) Flat-band diagram of alumina nanoparticles summarizing the relative energy positions of anion vacancies of different charge states, Al interstitial, and OH related/V type group of experimental data of this study and also the results of Refs. [3]–[61].

4. Conclusion and perspectives

In this study, various luminescence bands from NUV to the orange region were observed, followed by annealing treatment at 550 °C to 950 °C. While the positions of them remained unchanged (or with a small shift) after the calcination process, the absorption coefficient and integrated intensities for all luminescence bands were decreased due to rearrangement of atoms and a decrease in suspended and dangling bonds. In the presence of different kinds of defects, extra luminescence emissions were observed upon highly energetic excitation. The main intrinsic defects in the γ- and θ-alumina nanoparticles were oxygen vacancies in different charge states (F, F_2, F_2^+, and F_2^{2+} centers), cation interstitial, V-type hole centers related to cation vacancies or hole centers related to anion interstitial and OH related groups, which illustrated their approximate energy states. F and F_2 centers acted as sources of free electrons for the conduction band at excitation energies of about 6.05 and 5 eV, respectively. The excitation bands of surface OH groups or/and V type centers were located in the photoionization energies of F and F_2 centers. This means that the SRH recombination of dissociated electrons from F type centers to be captured by said hole centers or other delocalized holes in the place of said hole centers or in the place of donor–acceptor centers probably gave rise to the luminescence bands.

The photoionization energy threshold of F_2^+ centers was estimated to be a little smaller than 6.2 eV, which agreed exceptionally well with the absorption band of F centers while the photoionization thresholds of F_2 centers were estimated to be about 5 eV. F and F_2 centers played a crucial role in the photoconversion of other centers as well as the SRH recombination of carriers.

In nanostructures, there were two different types of F^+ centers, that is, the surface F^+ centers (F_S^+ centers) with an emission at 3.1–3.2 eV and the F^+ centers that are located in the bulk of nanostructures and have a similar trend to F^+ centers in the bulk materials with an emission of 3.8 eV. While the luminescence band of F_S^+ centers was detected, their excitation bands were strongly matched with F^+ center absorption bands, but the luminescence band of well localized F^+ centers (3.8 eV) was not recorded due to the following causes.

It is possible that all F^+ centers were located on the surface of nanoparticles and gave rise an emission at 3.1 eV. Or if this kind of defect was present in the structures of nanoparticles, then the relaxation process would be constituted by "non-radiative transitions". The mechanism of "non-irradiation excitation transfer between closely located F^+ and F centers "would be likely to take place or mechanism of possible" electron tunneling from F^+ to F centers" may occur.

A particularly interesting aspect of this study is associated with the observation of a lot of NUV–orange emission bands by a simple method. A survey of published spectra of Al_2O_3 in the literature shows that some new emission bands have been reported only by γ or neutron irradiations.

Acknowledgment

The authors are indebted to Iran's Nanotechnology initiative council for their financial support.

References

[1] Heimann R B 2010 *Classic and Advanced Ceramics: from Fundamentals to Applications* John Wiley & Sons
[2] Costina I and Franchy R 2001 *Appl. Phys. Lett.* **78** 4139
[3] Ealet B, Elyakhloufi M, Gillet E and Ricci M 1994 *Thin Solid Films* **250** 92
[4] Carrasco J, Gomes J R and Illas F 2004 *Phys. Rev. B* **69** 064116
[5] Aliabad H R 2015 *Chin. Phys. B* **24** 097102
[6] Guo Q L 2001 *Chin. Phys. B* 1080
[7] Ya-Bin W, Gang Z, Ming-Jie L, Xiang-Long C and Jun C 2009 *Chin. Phys. B* 181181
[8] Khatibani A B and Rozati S 2014 *Mater. Sci. Semicond. Process.* **18** 80
[9] Dhonge B P, Mathews T, Sundari S T, Thinaharan C, Kamruddin M, Dash S and Tyagi A 2011 *Appl. Surf. Sci.* **258** 1091
[10] Bouifoulen A, Edely M, Errien N, Kassiba A, Outzourhit A, Makowska-Janusik M, Gautier N, Lajaunie L and Oueriagli A 2011 *Thin Solid Films* **519** 2141
[11] Evans B D 1995 *J. Nucl. Mater.* **219** 202
[12] Gillet E and Ealet B 1992 *Surf. Sci.* **273** 427
[13] Boumaza A, Djelloul A and Guerrab F 2010 *Powder Technol.* **201** 177
[14] Kortov V, Ermakov A, Zatsepin A and Nikiforov S 2008 *Radiat. Meas.* **43** 341
[15] Trinkler L, Berzina B, Jakimovica D, Grabis J and Steins I 2010 *Opt. Mater.* **32** 789
[16] Surdo A, Kortov V and Pustovarov V 2001 *Radiat. Meas.* **33** 587
[17] Caulfield K J, Cooper R and Boas J F 1993 *Phys. Rev. B* **47** 55
[18] Springis M and Valbis J 1984 *Phys. Status Solidi (b)* **123** 335
[19] Ramírez R, Tardío M, González R, Munoz Santiuste J and Kokta M 2007 *J. Appl. Phys.* **101** 3520
[20] Ikeda S and Uchino T 2014 *J. Phys. Chem. C* **118** 4346
[21] Ramírez R, Tardío M, González R, Chen Y and Kokta M 2005 *Appl. Phys. Lett.* **86** 1914
[22] Carrasco J, Lopez N, Sousa C and Illas F 2005 *Phys. Rev. B* **72** 054109
[23] Kabler M, Crawford J and Slifkin L M 1972 *Plenum* New York 291
[24] Liu Y L, Liu G P, Wang W Y, Qi Z Q, Chen C Q and Wang Z G 2016 *Chin. Phys. B* **25** 87801
[25] Brewer J, Jeffries B and Summers G P 1980 *Phys. Rev. B* **22** 4900
[26] Perevalov T, Tereshenko O, Gritsenko V, Pustovarov V, Yelisseyev A, Park C, Han J H and Lee C 2010 *J. Appl. Phys.* **108** 013501
[27] Breysse M, Coudurier G, Claudel B and Faure L 1982 *J. Lumin.* **26** 239
[28] Malo M, Morono A and Hodgson E 2014 *Fusion Eng. Des.* **89** 2179
[29] Amirsalari A and Shayesteh S F 2015 *Superlattices Microstruct.* **82** 507
[30] Kulis P, Springis M, Tale I, Vainer V and Valbis J 1981 *Phys. Status Solidi (b)* **104** 719
[31] Kulis P, Springis M, Tale I and Valbis J 1980 *Phys. Status Solidi (a)* **58** 225
[32] Lee K H, Holmberg G and Crawford J 1977 *Phys. Status Solidi (a)* **39** 669
[33] Kortov V, Bessonova T, Akselrod M and Milman I 1985 *Phys. Status Solidi (a)* **87** 629
[34] Flerov A, Flerov V and Litvinov L 1991 *J. Appl. Spectrosc.* **54** 167
[35] Huang G, Wu X, Yang L, Shao X, Siu G and Chu P 2005 *Appl. Phys. A* **81** 1345
[36] El Mir L, Amlouk A and Barthou C 2006 *J. Phys. Chem. Solids* **67** 2395
[37] Trinkler L, Berzina B, Jakimovica D, Grabis J and Steins I 2011 *Opt. Mater.* **33** 817
[38] Gorbunov S, Cholakh S, Pustovarov V, Yakovlev V Y, Zatsepin A and Kucharenko A 2005 *Phys. Status Solidi (c)* **2** 351
[39] Li B, Hinklin T, Laine R and Rand S 2007 *J. Lumin.* **122** 345
[40] Pustovarov V, Aliev V S, Perevalov T, Gritsenko V and Eliseev A 2010 *J. Exp. Theor. Phys.* **111** 989
[41] Matsunaga K, Tanaka T, Yamamoto T and Ikuhara Y 2003 *Phys. Rev. B* **68** 085110
[42] Chen W, Song P, Dong Y, Zhang Y and Hua W 2013 *Chin. Sci. Bull.* **58** 1964
[43] Muthe K, Sudarshan K, Pujari P, Kulkarni M, Rawat N, Bhatt B and Gupta S 2009 *J. Phys. D: Appl. Phys.* **42** 105405
[44] Uenaka Y and Uchino T 2011 *Phys. Rev. B* **83** 195108
[45] Uzun E, Yarar Y and Yazici A N 2011 *J. Lumin.* **131** 2625
[46] Vreeker R, Kuzakov S and Glasbeek M 1985 *Solid State Commun.* **55** 1039
[47] Eglitis R, Kuklja M, Kotomin E, Stashans A and Popov A 1996 *Comput. Mater. Sci.* **5** 298
[48] Surdo A and Kortov V 2004 *Radiat. Meas.* **38** 667
[49] Stashans A, Kotomin E and Calais J L 1994 *Phys. Rev. B* **49** 14854
[50] Bartram R, Swenberg C and Fournier J 1965 *Phys. Rev.* **139** A941
[51] Sokol A A, Walsh A and Catlow C R A 2010 *Chem. Phys. Lett.* **492** 44
[52] Lee K, Holmberg G and Crawford J 1976 *Solid State Commun.* **20** 183
[53] Rao T G, Bhatt B and Page P 2008 *Radiat. Meas.* **43** 295
[54] El-Mansy M, Diefallah E and Shash N 1995 *Radiat. Phys. Chem.* **45** 151
[55] Varley J, Janotti A, Franchini C and Van de Walle C 2012 *Phys. Rev. B* **85** 081109
[56] Jacobs P W and Kotomin E A 1994 *J. Am. Ceram. Soc.* **77** 2505
[57] Otto T N 2013 *Optoelectronic Properties of Lead Selenide Quantum Dot Thin Films*
[58] Li Z and Huang K 2007 *J. Lumin.* **127** 435
[59] Ortiz A, Alonso J, Pankov V and Albarran D 1999 *J. Lumin.* **81** 45
[60] Shen Y F, Suib S L, Deeba M and Koermer G 1994 *J. Catal.* **146** 483
[61] Stoyanovskii V and Snytnikov V 2009 *Kinet. Catal.* **50** 450